

Spatial and Temporal Excitation to Generate Traveling Waves in Structures

Ran Gabai

Dynamics Laboratory,
Faculty of Mechanical Engineering,
Technion IIT,
Technion City, Haifa, 32000, Israel
e-mail: rang@technion.ac.il

Izhak Bucher

Head of the Dynamics Laboratory,
Faculty of Mechanical Engineering,
Technion IIT,
Technion City, Haifa, 32000, Israel
e-mail: bucher@technion.ac.il

The problem in the creation of traveling waves is approached here from an unconventional angle. The formulation makes use of normal vibration modes, which are standing waves, to express both traveling waves and the required force distribution. It is shown that a localized force is required at any discontinuity along the structure to absorb reflected waves. This convention is demonstrated for one- and two-dimensional structures modeled as continua, and as discretized numerical approximation of the mass and stiffness matrices. Harmonic vibrations can be characterized as standing or traveling waves or as a combination of both. By applying forces that have been specially designed for the purpose, the vibratory response can become a pure traveling wave. The force distribution is important for the design of ultrasonic motors and in control applications, attempting to absorb and create outgoing and incoming waves. [DOI: 10.1115/1.3176999]

1 Introduction

Pure traveling vibration waves are seldom observed on passive finite structures [1]. Traveling deformation waves create propulsion, e.g., ultrasonic motors [2]; squeeze-film levitation and transportation devices [3], where a traveling pressure wave carries a levitated object in the direction the wave progresses; and in robotics where a snakelike structure exhibits traveling wave movements to create propulsion, steering and maneuvering in a viscous fluid environment [4]. Traveling wave type of modeling can be used for closed loop control and modeling [5]. Common methods for generating traveling waves in structures are the two-mode excitation [2], where two modes having close natural frequencies can be combined to form an approximate traveling wave. A different approach, the “active-sink” method [6], employs two actuators that are being used to simultaneously excite and absorb the traveling wave, thus preventing reflection from the boundaries of the structure. Waves at steady-state have been used to actively damp vibrations in flexible structures [7]. In Refs. [5,8], a traveling wave approach was used for closed loop position control.

In this work, one-dimensional structures such as strings and beams, and two-dimensional membranes are considered. The generation of traveling waves in strings and beams was implemented with the active-sink method [6,9,10]. In 2D, the two-modes excitation approach has been employed in Ref. [11].

The methods above constrain the actuators to be located at the structure boundaries. This seems reasonable from the perspective of achieving matched impedances at the boundaries, but no mathematical proof has been presented so far to justify this choice. The present work does not assume any prior knowledge on the spatial distribution of external loads. Rather, it formulates a mathematical problem whose solution determines the force deployment under which a traveling wave is formed. A modal approach, which uses the normal modes—i.e., standing waves, is being used to represent the traveling waves. The obtained results support, in several cases, the common practice that forces should act at the boundaries. These results are extended to more complicated cases. An extension to the case where a discontinuity is present shows that additional forces are required. Some cases are demonstrated numerically via finite element models and by using matrix algebra.

Working with waves and vibrations, it is necessary to decompose the motion into the traveling and standing components. Several methods have been proposed for this purpose, fitting the measured complex amplitude by an ellipse performs this task in one-dimensional structure [12], another method uses the proper orthogonal decomposition (POD) [13], and finally, an approximation of the power-flow may also be used for this purpose [14].

The paper initially develops the proposed method analytically for a taut string, and investigates the results. Then, the method is expanded for a general discrete system. Next, several cases of one and two-dimensional structures are studied.

2 Computing the Required Force Distribution to Create Traveling Waves in a Taut String

Many vibration problems are being solved when the spatial force distribution is known; the problem at hand is different from this perspective. In order to create a specific spatial and temporal behavior, forces may be required at every point along the structure. The question being answered here, analytically, refers to the required force deployment for the creation of traveling waves that move at their characteristic speed while being driven at a single frequency. In this section, the distribution of external forces that generate traveling waves with a given wavelength is found. The force and response distributions are described in terms of a summation of the natural modes and the contribution of each mode to the response, and later to the force distributions are derived. First, the question of how should the forces be distributed along the structure is being answered.

2.1 Calculating the Required Excitation Using an Infinite Modal Summation: An Analytical Solution. Considering a taut string, with length L , cross section area A , and density ρ . The string experiences a constant tension force T , and it is subjected to a body force $f(x,t)$. Its deflection is denoted by $u(x,t)$ and the equation of motion is described by the one-dimensional forced wave equation [15],

$$\rho A \frac{\partial^2 u}{\partial t^2} - T \frac{\partial^2 u}{\partial x^2} = f(x,t) \quad (1)$$

Additionally, the wave velocity is defined as follows:

$$c = \sqrt{\frac{T}{\rho A}} \quad (2)$$

Contributed by the Applied Mechanics Division of ASME for publication in the JOURNAL OF APPLIED MECHANICS. Manuscript received December 14, 2008; final manuscript received March 26, 2009; published online December 11, 2009. Review conducted by Professor Sridhar Krishnaswamy.

It is possible to define nondimensional coordinates ξ, τ via

$$\xi = \frac{x}{L}, \quad \tau = \frac{c}{L}t \quad (3)$$

with this transformation, Eq. (1) becomes nondimensional, i.e.,

$$\frac{\partial^2 u}{\partial \tau^2} - \frac{\partial^2 u}{\partial \xi^2} = \tilde{f}(\xi, \tau) \quad (4)$$

where

$$\tilde{f}(\xi, \tau) = \frac{L}{T} f(x, t) \quad (5)$$

Using Eq. (4), the nondimensional wave velocity becomes unity. The normal modes of the string can be described by [15]

$$\phi_n(\xi) = C_n(e^{-i\beta_n \xi} + e^{i\beta_n \xi}) + iD_n(e^{-i\beta_n \xi} - e^{i\beta_n \xi}) \quad (6)$$

where

$$\beta_n = \frac{\omega_n}{c} \quad (7)$$

The natural frequencies, ω_n , depend on the boundary conditions. A general solution of Eq. (4) can be expressed as an infinite summation of modes:

$$u_{\text{modes}} = \sum_{n=1}^{\infty} \phi_n(\xi) \eta_n(\tau) \quad (8)$$

where $\eta_n(\tau)$ are the modal coordinates.

In order to impose a traveling wave response, one has to select either the excitation frequency (ω), or the wavenumber (κ) that dictates the wavelength (λ), via

$$\kappa = \frac{2\pi}{\lambda} \quad (9)$$

The desired response of a pure traveling wave in the positive direction is given by

$$u_{tw}(\xi, \tau) = C_0 e^{-i(\kappa \xi - \omega \tau)} \quad (10)$$

Next, the traveling wave will be decomposed in terms of the natural modes.

2.1.1 Describing a Traveling Wave Using a Modal Summation. In order to describe the desired traveling wave solution in terms of the string modes, a least-squares error function, J , is introduced as follows:

$$J = \int_0^1 \left(u_{tw}(\xi, \tau) - \sum_{n=1}^{\infty} \phi_n(\xi) \eta_n(\tau) \right)^2 d\xi \quad (11)$$

The modal coordinates that minimize or nullify Eq. (11) are obtained by differentiating with respect to the modal coordinates

$$\frac{\partial J}{\partial \eta_m(\tau)} = \int_0^1 2 \left(u_{tw}(\xi, \tau) - \sum_{n=1}^{\infty} \phi_n(\xi) \eta_n(\tau) \right) \phi_m(\xi) d\xi = 0 \quad (12)$$

Rearranging

$$\int_0^1 u_{tw}(\xi, \tau) \phi_m(\xi) d\xi = \eta_m(\tau) \int_0^1 \sum_{n=1}^{\infty} \phi_n(\xi) \phi_m(\xi) d\xi \quad (13)$$

Due to the orthogonality of the modes [16], the integral on the right hand side of Eq. (13) equals to zero for all $n \neq m$. Equation (13) thus becomes

$$\int_0^1 u_{tw}(\xi, \tau) \phi_m(\xi) d\xi = \eta_m(\tau) \int_0^1 \phi_m^2(\xi) d\xi \quad (14)$$

The optimal (in the least-squares sense) modal coordinates η_m , describing the modal representation of the desired traveling wave, can be found from

$$\eta(\tau) = \frac{\int_0^1 u_{tw}(\xi, \tau) \phi_m(\xi) d\xi}{\int_0^1 \phi_m^2(\xi) d\xi} \quad (15)$$

It is now possible to obtain an expression for the modal coordinates when the response is a traveling wave (the one shown in Eq. (10)):

$$\eta_m(\tau) = \frac{4C_0\beta_n e^{2i\beta_n \tau} [(\cos(\beta_n) e^{-i\kappa} - 1)(i\kappa C_n + \beta_n D_n) + i \sin(\beta_n) e^{-i\kappa} (i\beta_n C_n + \kappa D_n)] e^{i\omega \tau}}{(\kappa^2 - \beta_n^2) [4(C_n D_n + \beta_n (C_n^2 + D_n^2)) e^{2i\beta_n} - C_n D_n (2 + e^{4i\beta_n}) + i(C_n^2 - D_n^2)(1 - e^{4i\beta_n})]} \quad (16)$$

Clearly many, if not all the modes, that are in fact standing waves, participate in creating the traveling wave. The role of the different modes will be investigated below.

2.1.2 Calculating the Necessary Forces. Now, the external forces, $\tilde{f}(\xi, \tau)$, that would create the traveling wave $u_{tw}(\xi, \tau)$ can be found. The forces can be described as a weighted sum of modal vectors (functions), since the modal functions create a complete basis as follows:

$$f(\xi, \tau) = \sum_{n=1}^{\infty} \phi_n(\xi) \alpha_n(\tau) \quad (17)$$

By calculating the coefficients, $\alpha_n(\tau)$, the force distribution can be obtained. Substituting the traveling wave solution in Eq. (10) and the force in Eq. (17) into the equation of motion (Eq. (1)), one obtains

Building another least-squares type of error function:

$$\sum_{n=1}^{\infty} \phi_n(\xi) \ddot{\eta}_n(\tau) - \sum_{n=1}^{\infty} \frac{d^2}{d\xi^2} \phi_n(\xi) \eta_n(\tau) = \sum_{n=1}^{\infty} \phi_n(\xi) \alpha_n(\tau) \quad (18)$$

$$J_F = \int_0^1 \left(\sum_{n=1}^{\infty} \phi_n(\xi) \ddot{\eta}_n(\tau) - \sum_{n=1}^{\infty} \frac{d^2}{d\xi^2} \phi_n(\xi) \eta_n(\tau) - \sum_{n=1}^{\infty} \phi_n(\xi) \alpha_n(\tau) \right)^2 dx \quad (19)$$

and finding the coefficients that minimize J_F (by differentiating it with respect to α_m):

$$\frac{\partial J_F}{\partial \alpha_m} = \int_0^1 2 \left(\sum_{n=1}^{\infty} \phi_n(\xi) \ddot{\eta}_m(\tau) - \sum_{n=1}^{\infty} \frac{d^2}{d\xi^2} \phi_n(\xi) \eta_n(\tau) - \sum_{n=1}^{\infty} \phi_n(\xi) \alpha_n(\tau) \right) \phi_m(\xi) d\xi = 0 \quad (20)$$

Once again, using the orthogonality of the modes, one obtains

$$\alpha_m(\tau) \int_0^1 \phi_m^2 d\xi = \ddot{\eta}_m(\tau) \int_0^1 \phi_m^2 d\xi - \eta_m(\tau) \int_0^1 \phi_m \frac{d^2}{d\xi^2} \phi_m(\xi) d\xi \quad (21)$$

It proves helpful to use the fact that the mode shapes comply with [17]:

$$\frac{d^2 \phi_m}{d\xi^2} = -\beta_m^2 \phi_m \quad (22)$$

$$\int_0^1 \phi_m \frac{d^2 \phi_m}{d\xi^2} d\xi = -\beta_m^2 \int_0^1 \phi_m^2 d\xi$$

Substituting Eq. (22) into Eq. (21), and using the fact that $\dot{\eta}_m(\tau) = -\omega^2 \eta_m(\tau)$, the coefficients $\alpha_m(\tau)$ become

$$\alpha_m(\tau) = (\omega_m^2 - \omega^2) \eta_m(\tau) \quad (23)$$

Finally, substituting the modal coordinates in Eq. (15) into Eq. (23), one obtains

$$\alpha_m(\tau) = (\omega_m^2 - \omega^2) \frac{\int_0^1 u_{tw}(\xi, \tau) \phi_m(\xi) d\xi}{\int_0^1 \phi_m^2(\xi) d\xi} \quad (24)$$

Equation (24) provides a closed form expression for the forces required to create any type of desired response. In the particular case of a traveling wave, substituting Eq. (16) into Eq. (24), one obtains

$$\alpha_n(\tau) = \frac{-4C_0 B_n e^{2i\beta_n} [(\cos(\beta_n) e^{-i\kappa} - 1)(i\kappa C_n + \beta_n D_n) + i \sin(\beta_n) e^{-i\kappa} (i\beta_n C_n + \kappa D_n)] e^{i\omega\tau}}{[4(C_n D_n + \beta_n(C_n^2 + D_n^2)) e^{2i\beta_n} - C_n D_n (2 + e^{4i\beta_n}) + i(C_n^2 - D_n^2)(1 - e^{4i\beta_n})]} \quad (25)$$

Having found the required force, it is now possible to calculate the external force's distribution. This is carried out below for several cases.

2.2 Analytical Solution of the Required Forces for a Free-Free String. The simplest theoretical example presented here deals with an unsupported taut string. Such a string has natural frequencies equal to

$$\omega_n = n\pi, \quad n = 0, 1, 2, \dots$$

and eigenfunctions (modes)

$$\phi_n(\xi) = e^{-i\pi n \xi} + e^{i\pi n \xi}, \quad n = 0, 1, 2, \dots \quad (26)$$

The string's response is described as a modal summation (including the rigid body mode):

$$\tilde{u}(\xi, \tau) = \sum_{n=0}^{\infty} \eta_n(\tau) \phi_n(\xi) \quad (27)$$

Substituting Eqs. (10) and (26) into Eq. (15), the modal coordinates are obtained as follows:

$$\eta_n(\tau) = \frac{i\kappa}{\kappa^2 - n^2 \pi^2} [-1 + (-1)^n e^{-i\kappa}] e^{i\omega\tau} \quad (28)$$

The distributed force that needs to be applied to the string is also described by a modal summation:

$$\tilde{f}(\xi, \tau) = \alpha_0(\tau) \phi_0(\xi) + \sum_{n=1}^{\infty} \alpha_n(\tau) \phi_n(\xi) \quad (29)$$

The component $\alpha_0 \phi_0$ represents a constant force arising due to the free boundary conditions. Using Eq. (23), the modal force's coefficients $-\alpha_n(\tau)$ can be computed as follows:

$$\alpha_n(\tau) = (n^2 \pi^2 - \kappa^2) \eta_n(\tau) = i\kappa [1 - (-1)^n e^{-i\kappa}] e^{i\omega\tau} \quad (30)$$

Substituting Eq. (30) and the modes (Eq. (26)) into Eq. (29), a seemingly complicated expression is found as follows:

$$\begin{aligned} \tilde{f}(\xi, \tau) &= \alpha_0 \phi_0 + i\kappa e^{i\omega\tau} \sum_{n=1}^{\infty} [1 - (-1)^n e^{-i\kappa}] (e^{-i\pi n \xi} + e^{i\pi n \xi}) \\ &= \alpha_0 \phi_0 + i\kappa e^{i\omega\tau} \left[\sum_{n=1}^{\infty} (e^{-i\pi n \xi} + e^{i\pi n \xi}) - e^{-i\kappa} \sum_{n=1}^{\infty} (-1)^n (e^{-i\pi n \xi} + e^{i\pi n \xi}) \right] \quad (31) \end{aligned}$$

This expression, once simplified, provides an insight into the general shape of the solution. Below, some mathematical simplifications are employed to produce this insight.

Handling the $(-1)^n$ expression in Eq. (31) by separating it into the sum of even n 's ($n=2m$) and odd n 's ($n=2p-1$):

$$\tilde{f}(\xi, \tau) = \alpha_0 \phi_0 + i\kappa e^{i\omega\tau} \left[\sum_{n=1}^{\infty} \overbrace{(e^{-i\pi n \xi} + e^{i\pi n \xi})}^{S_1} - e^{-i\kappa} \sum_{m=1}^{\infty} \overbrace{(e^{-i\pi 2m \xi} + e^{i\pi 2m \xi})}^{S_2} + e^{-i\kappa} \sum_{p=1}^{\infty} \overbrace{(e^{-i\pi(2p-1)\xi} + e^{i\pi(2p-1)\xi})}^{S_3} \right] \quad (32)$$

Working on each of the sums by itself, and using the identity [18]:

$$\sum_{n=-\infty}^{\infty} e^{2\pi i n y} = \sum_{n=-\infty}^{\infty} \delta(y - n) \quad (33)$$

where $\delta(y)$ is the Dirac delta function, simplifying the sums S_1, S_2, S_3 as follows:

$$S_1 = \sum_{n=1}^{\infty} (e^{-i\pi n \xi} + e^{i\pi n \xi}) = -2 + \sum_{n=-\infty}^{\infty} e^{i\pi n \xi} = -2 + \sum_{n=-\infty}^{\infty} \delta(\xi - 2n) \quad (34)$$

$$S_2 = \sum_{m=1}^{\infty} (e^{-i\pi 2m \xi} + e^{i\pi 2m \xi}) = -2 + \sum_{m=-\infty}^{\infty} e^{i\pi 2m \xi} = -2 + \sum_{m=-\infty}^{\infty} \delta(\xi - m) \quad (35)$$

$$\begin{aligned} S_3 &= \sum_{p=1}^{\infty} (e^{-i\pi(2p-1)\xi} + e^{i\pi(2p-1)\xi}) = \sum_{p=-\infty}^{\infty} e^{i\pi(2p-1)\xi} \\ &= \sum_{p=-\infty}^{\infty} \delta\left(\xi - \frac{2p^2}{2p-1}\right) \end{aligned} \quad (36)$$

Now, since $\xi \in (0, 1)$, the expressions for S_1, S_2, S_3 inside the domain degenerate into

$$\begin{aligned} S_1 &= -2 + \delta(\xi) \\ S_2 &= -2 + \delta(\xi) + \delta(\xi - 1) \\ S_3 &= \delta(\xi) \end{aligned} \quad (37)$$

and the rigid body mode's contribution is

$$\alpha_0 \phi_0 = 2i\kappa[1 - e^{-i\kappa}]e^{i\omega\tau} \quad (38)$$

Substituting Eqs. (37) and (38) into Eq. (32) one finally obtains

$$\begin{aligned} \tilde{f}(\xi, \tau) &= \alpha_0 \phi_0 + i\kappa e^{i\omega\tau}[-2 + \delta(\xi) - e^{-i\kappa}[-2 + \delta(\xi) + \delta(\xi - 1) \\ &\quad + e^{-i\kappa} \delta(\xi)]] = i\kappa e^{i\omega\tau}[\delta(\xi) - e^{-i\kappa} \delta(\xi - 1)] \end{aligned} \quad (39)$$

Equation (39) shows that only two point forces need to be applied to create a traveling wave on a uniform string. These forces are located at the edges of the string. Mathematically, the force distribution, in space and time, can be expressed as

$$f(\xi, \tau) = F_1 \delta(\xi) e^{i\omega\tau} + F_2 \delta(\xi - 1) e^{i\omega\tau} \quad (40)$$

After it has been established mathematically that the forces should be applied only to the edges, it is possible to calculate the magnitude of these forces for a desired traveling wave in a direct manner, using the active-sink method [6], such a solution is detailed in Ref. [9]. Here, only the final result is provided for comparison.

The forces applied to the string's edges ($f_1(\tau), f_2(\tau)$) can be expressed as boundary conditions

$$\begin{aligned} \frac{\partial^2 u}{\partial \tau^2} - \frac{\partial^2 u}{\partial \xi^2} &= 0 \\ \frac{\partial u}{\partial \xi} \Big|_{\xi=0} &= -f_1 e^{i\omega\tau} \\ \frac{\partial u}{\partial \xi} \Big|_{\xi=1} &= f_2 e^{i\omega\tau} \end{aligned} \quad (41)$$

Imposing a pure traveling wave solution as was carried out in Ref. [9] (e.g., substitute Eq. (10) into Eq. (41)), the ratio between the forces f_1, f_2 can be calculated [9] as follows:

$$\frac{f_2}{f_1} = -e^{-i\kappa} \quad (42)$$

Indeed, this result is identical to what was obtained in Eq. (39).

2.2.1 Exciting Traveling Waves at Resonance. It is well known that when a structure is excited sinusoidally close to resonance, the prevailing response consists of a standing wave that is proportional to the corresponding eigenfunction. Exciting a model without damping of such a structure, at one of its natural frequencies, results in an unbounded solution. The question arises, what happens when one tries to generate a traveling wave close to a natural frequency? With the absence of damping in the model, it is possible to check the solution by producing a slightly detuned natural wavenumber (or natural frequency):

$$\kappa = \beta_n + \varepsilon \quad (43)$$

The n th mode's amplitude, η_n , is the one expected to become unbounded since it has the term $(\kappa - \beta_n)$ in its denominator. Substituting the detuned wavenumber from Eq. (43) into η_n and expanding to a Taylor series around $\varepsilon=0$ reveals the fact that

$$\eta_n = \text{const} + O(\varepsilon) \quad (44)$$

This means that a traveling wave in the vicinity of a natural frequency has finite amplitude. Despite the high compliance of the structure at this frequency, much of the energy that is pumped in by the actuation is carried away by the traveling wave itself and being sucked out by the applied forces at the appropriate location.

It can be concluded that suitable boundary control can potentially alleviate resonance problems by absorbing the, otherwise circulating, energy.

3 Computing the Required Force Distribution to Create Traveling Waves in Discrete Systems

The method which was demonstrated on continuous structures in Sec. 2 can be expanded to deal with general discrete dynamical systems having inertia and stiffness matrices \mathbf{M}, \mathbf{K} , respectively, and where a generalized vector of forces \mathbf{F} act on this structure. Such a system is described by a second order vector equation of motion having N degrees of freedom contained in $q(t)$,

$$\mathbf{M}\ddot{q} + \mathbf{K}q = \mathbf{F} \quad (45)$$

Solving the generalized eigenvalues problem of \mathbf{K}, \mathbf{M} , the normal modes, ϕ_n , and natural frequencies, ω_n , of the system are calculated and assembled into the modal matrix, Φ ,

$$\Phi = [\phi_1 \quad |\phi_2| \quad \cdots \quad |\phi_N] \quad (46)$$

and into a diagonal matrix Λ :

$$\Lambda = \begin{bmatrix} \omega_1^2 & & \\ & \ddots & \\ & & \omega_N^2 \end{bmatrix} = (\Phi^T \mathbf{M} \Phi)^{-1} (\Phi^T \mathbf{K} \Phi) \quad (47)$$

3.1 Calculating the Modal Coordinates. The response of the system may be described as a modal summation:

$$q(t) = \sum_{n=1}^N \phi_n(x) \eta_n(t) = \Phi \boldsymbol{\eta} \quad (48)$$

where η_n are the modal coordinates and

$$\boldsymbol{\eta} = [\eta_1(t) \quad \eta_2(t) \quad \cdots \quad \eta_N(t)]^T \quad (49)$$

Denoting the desired traveling wave solution as $q_{tw}(x, t)$, it can be expressed as a combination of the system modes,

$$q_{tw}(x, t) = \Phi \boldsymbol{\eta}_{tw} \quad (50)$$

where $\boldsymbol{\eta}_{tw}$ is a vector of the modal coordinates describing the desired response. Since the modal matrix Φ is bi-orthogonal with respect to \mathbf{M} it is possible to calculate Φ^{-1} as follows:

$$\Phi^{-1} = (\Phi^T \mathbf{M} \Phi)^{-1} \Phi^T \mathbf{M} \quad (51)$$

This allows one to calculate η_{tw} in Eq. (50),

$$\eta_{tw}(t) = (\Phi^T \mathbf{M} \Phi)^{-1} (\Phi^T \mathbf{M} q_{tw}) \quad (52)$$

The expression obtained in Eq. (52) is the discrete version of the expression that was developed for the continuous systems in Sec. 2.1 (Eq. (15)).

3.2 Calculating the Required Forces. The normal modes, ϕ_n , span \mathbb{R}^N , thus, \mathbf{F} can be expressed as [19,20]

$$\mathbf{F} = \mathbf{M} \Phi \boldsymbol{\alpha}(t) \quad (53)$$

where

$$\boldsymbol{\alpha}(t) = [\alpha_1(t) \quad \alpha_2(t) \quad \cdots \quad \alpha_N(t)]^T$$

and $\alpha_n(t)$ are the coefficients of the modal forces [20]. Substituting Eqs. (50)–(53) into Eq. (45) and left multiplying by Φ^T ,

$$\Phi^T \mathbf{M} \Phi \ddot{\eta}_{tw} + \Phi^T \mathbf{K} \Phi \eta_{tw} = \Phi^T \mathbf{M} \Phi \boldsymbol{\alpha}(t) \quad (54)$$

Left multiplying Eq. (54) by the expression $(\Phi^T \mathbf{M} \Phi)^{-1}$, Eq. (54) becomes

$$\ddot{\eta}_{tw}(t) + \Lambda \eta_{tw}(t) = \boldsymbol{\alpha}(t) \quad (55)$$

Since $\ddot{\eta}_{tw} = -\omega^2 \eta_{tw}$, the coefficients can be calculated via

$$\boldsymbol{\alpha}(t) = (\Lambda - \mathbf{I} \omega^2) \boldsymbol{\eta}_{tw}(t) \quad (56)$$

$$\alpha_n(t) = (\omega_n^2 - \omega^2) \eta_{tw,n}(t)$$

Substituting Eq. (56) into Eq. (53), the forces can be calculated as follows:

$$\mathbf{F}(t) = \mathbf{M} \Phi (\Lambda - \mathbf{I} \omega^2) \boldsymbol{\eta}_{tw}(t) = \mathbf{M} \Phi (\Lambda - \mathbf{I} \omega^2) (\Phi^T \mathbf{M} \Phi)^{-1} (\Phi^T \mathbf{M} q_{tw}) \quad (57)$$

The expression obtained in Eq. (57) is the discrete equivalent of Eq. (24) calculated in Sec. 2.1. Using Eq. (57), the forces that generate a traveling wave can be computed. The magnitude and phase shift of all forces that should be applied to the structure depend on the desired response, as evident in Eq. (57). Also, the expression given in Eq. (52) shows the participation level of each mode in forming the traveling wave. Using these expressions, the distribution and time variation in the forces can be computed. The newly introduced equations are employed in several cases to shed some light on the physical meaning of the results.

3.3 Using Partial Modal Summation. Sometimes, only a limited number of modes is known. This is especially true for very large models, or for models obtained from measurements. Moreover, the modes whose corresponding natural frequency is close to the excitation frequency carry much more power than far away modes. Thus, there is a group of modes that dominates the structure's response. A truncated modal matrix built from a group of the relevant modes, $\bar{\Phi}$, and $\bar{\Lambda}$ composed only from the relevant eigenfrequencies can thus be used instead of the full modal matrix in Eqs. (52) and (57) in order to calculate the required forces:

$$\eta_{tw}(t) = (\bar{\Phi}^T \bar{\mathbf{M}} \bar{\Phi})^{-1} (\bar{\Phi}^T \bar{\mathbf{M}} q_{tw}) \quad (58)$$

$$\mathbf{F}(t) = \mathbf{M} \bar{\Phi} (\bar{\Lambda} - \mathbf{I} \omega^2) (\bar{\Phi}^T \bar{\mathbf{M}} \bar{\Phi})^{-1} (\bar{\Phi}^T \bar{\mathbf{M}} q_{tw})$$

The forces calculated in Eq. (58) are designed to excite only the selected modes in $\bar{\Phi}$. This means that a response composed from fewer modes can describe a pseudo-traveling-wave response and may be considered as an extension of the two-mode excitation method [2].

4 Case Studies

This section studies the results of the presented method by calculating the excitation required to obtain traveling waves in common structures. A beam is used to study one-dimensional waves

and a membrane is being used for the two-dimensional case. The role of evanescent waves in the beam and the ability to control their effect is also studied.

4.1 Creating Waves in an Euler–Bernoulli Beam. Considering an Euler–Bernoulli beam, having ρ, A, E, I that are density, cross area section, module of elasticity, and moment of inertia, respectively. The beam's deflection is $w(x, t)$, and both external forces $f(x, t)$ and external moments $m(x, t)$ may be applied to this model. The equation of motion is [21]:

$$\rho A \frac{\partial^2 w}{\partial t^2} + EI \frac{\partial^4 w}{\partial x^4} = f(x, t) - \frac{\partial m(x, t)}{\partial x} \quad (59)$$

It is possible to find the forces that excite any combination of traveling and standing waves, in the same manner it was shown in Sec. 2. A complete solution of the beam vibrations contains also evanescent waves, thus,

$$w(x, t) = (C_1 e^{-i\kappa x} + C_2 e^{i\kappa x} + C_3 e^{-\kappa x} + C_4 e^{\kappa x}) e^{i\omega t} \quad (60)$$

The relationship between the excitation frequency ω and the obtained wavenumber κ is [15]

$$\kappa = \sqrt{\frac{EI}{\rho A} \omega^4} \quad (61)$$

Here, to overcome the analytical obscurity of the lengthy expressions, the beam is modeled using finite elements (FE), and a discrete model (such as given in Eq. (45)) is being employed.

The generalized coordinates of this model contain both the deflection and the bending angle of each node [22]. Thus, it is possible to apply both a point force and pure moment to each node independently. Using the results of Sec. 3, and simulating an FE model of a beam, it is possible to calculate the forces which excite a pure traveling wave in the beam.

For the simulation, a steel beam ($\rho=7800 \text{ kg/m}^3$, $E=210 \text{ GPa}$) of length $L=1 \text{ m}$ having cross area section $A=3.0784 \times 10^{-6} \text{ m}^2$ and moment of inertia $I=6.9367 \times 10^{-14} \text{ m}^4$, is modeled. The beam is held by flexible supports at both ends. Using Eq. (52), where q_{tw} is formed to describe a pure traveling wave, the modal coordinates $\eta_n(t)$ are calculated.

In Fig. 1, the amplitude of the modal coordinates ($|\eta_n|$) is shown for two different sets of q_{tw} having different wavelengths. It is seen that a group of modes having a natural frequency close to the excitation frequency have the largest contribution. Looking over the expression for η , obtained analytically for the string in Sec. 2.1.1, which ought to have a similar structure for a beam, either the term $(\kappa^2 - \beta_n^2)$ or $(\omega^2 - \omega_n^2)$ appears in the denominator. This means that wavelengths that are close to the natural wavelengths of the modes have higher gain.

Using Eq. (57), the force distribution needed to be applied to the beam is calculated. It is revealed that both forces and moments must be applied to the beam to achieve a desired traveling wave response as was previously reported in Refs. [9,10]. The left part of Fig. 2 shows the forces and moments that should be applied to the beam to create a desired traveling wave when considering all of the modes of the structure. It can be seen that the result indeed sums up to localized forces and moments at the edges of the beam. Also, the results show that the amplitude of the forces and moments on one end are identical to the forces and moments at the other end of the beam. This is so since the boundary conditions being used in this simulation are identical [9]. This result also explains the fact that a pure traveling wave response of a beam cannot be achieved by applying only forces. Therefore moments are required to accommodate the evanescent waves [9]. This result can explain why two closely spaced forces should be placed at the absorbing end of a structure when waves should be completely absorbed [8].

4.1.1 Using a Subset of the Modes. As shown in Fig. 1, the contribution of the majority of the modes to the traveling wave

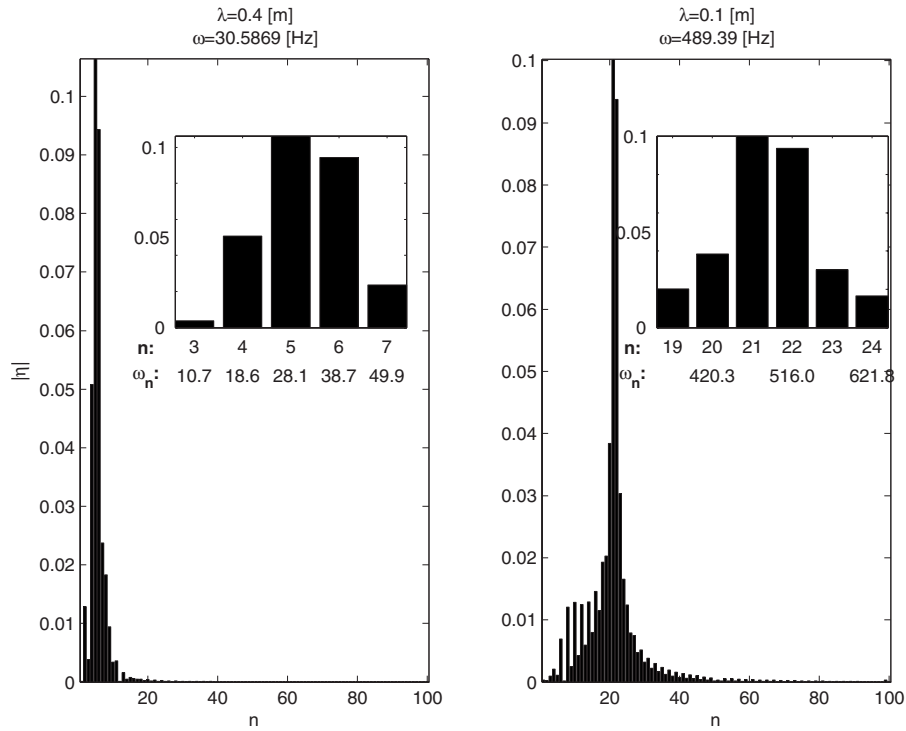


Fig. 1 Modal coordinates describing a pure traveling wave having different wavelengths. (Left) $\lambda=0.4$ m and (right) $\lambda=0.1$ m. Small windows show an enlarged portion of most contributing coefficients.

response is insignificant compared with the contribution from modes whose natural frequencies are close to the excitation frequency. This may tempt the designer to choose a limited set of modes to perform the required calculations.

The effect of a truncated model is examined with the same beam example from Sec. 4.1. A traveling wave with wavelength $\lambda=0.4$ m with a truncated model containing only the first ten

modes of the beam to calculate the needed forces is simulated.

The right hand side of Fig. 2 shows the resulting force distribution in space and time. It can be seen that rather than a localized point force and moment at the edge of the beam, spatially distributed forces and moments along the beam are required in this case. Figure 3 shows that the evolution of the deformation along the beam is in fact a traveling wave. It is seen that although the force

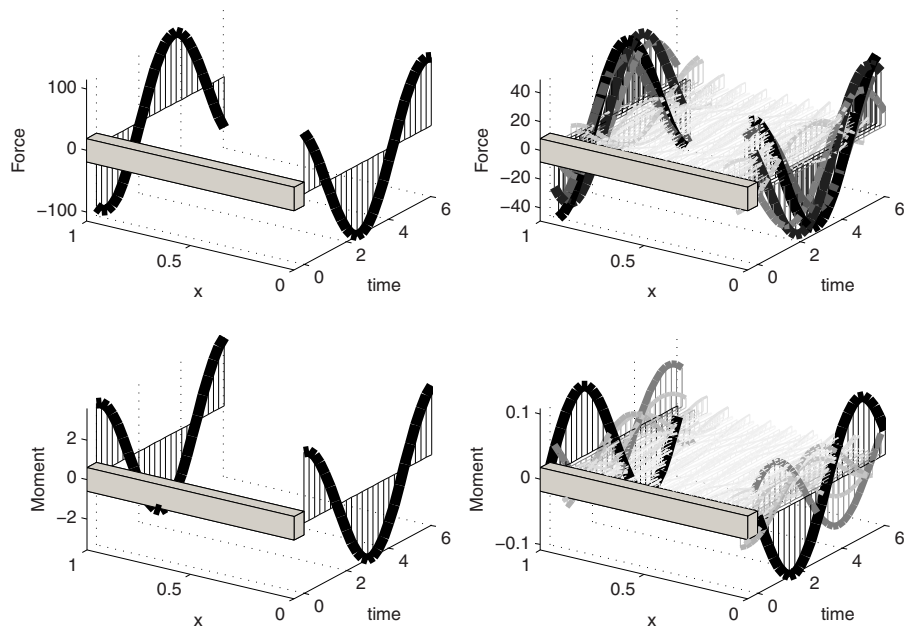


Fig. 2 Spatial distribution of forces and moments applied to a beam to achieve a pure traveling wave ($\lambda=0.4$ m) (left) using all the modes to calculate the forces, (right) using only the first ten modes of the beam, (top) force distribution, and (bottom) moment distribution

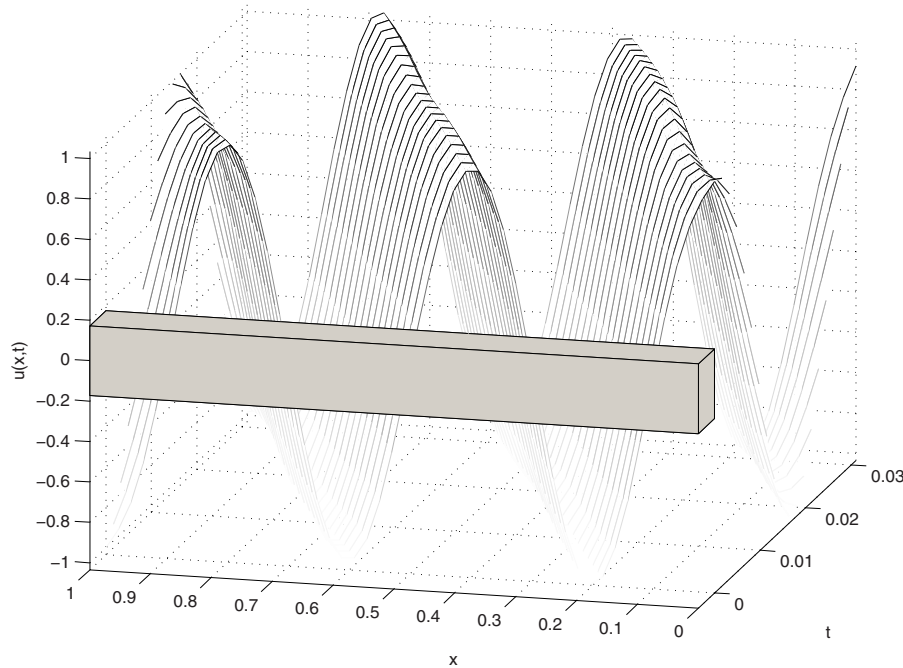


Fig. 3 Illustration of the beam response in time and space when using only the first ten modes to describe the desired traveling wave response

distribution is significantly different from the forces calculated for the full model (using all of the modes), the response is still very close to a traveling wave.

4.1.2 The Effect of Spatially Selective or Truncated Excitation. Occasionally, a beam is excited using forces (or moments) alone (for example in Refs. [2,6]). According to the results of Sec. 4.1, it is not possible to achieve pure traveling waves along the beam without using both forces and moments. Referring to the excitation that achieves the exact solution as the optimal excitation, this section investigates the effect of applying a suboptimal excitation. In order to assess how pure is the obtained wave, it is possible to inspect the nature of the response in the complex plane [9,10,12]. In general, the complex response amplitude, along the structure, traces an ellipse, when a single wavelength appears in the response. The closer the response is to a traveling wave, the more it resembles a circle. Alternatively, when the response becomes a standing wave, the ellipse becomes elongated until it approaches a straight line.

In order to evaluate the contribution of the moments to the purity of the traveling waves, Eq. (58) has been employed, but only the linear forces were considered in the simulation (the moments were forced to be zero). With only point forces acting on the structure, the beam's response was computed. As expected, the beam's response is not a pure traveling wave, but a mixture of traveling and standing waves. Figure 4 compares the beam's response to the optimal excitation (i.e., forces and moments) with the response to forces only. While the complex amplitude of the response to the optimal excitation falls on a perfect circle in the complex plane, the response to the reduced excitation traces a part that resembles an ellipse in the center of the beam and a much longer wavelength [12] close to the edges of the beam. Indeed, the response closer to the beam's edges is related to the evanescent waves' part of the beam's forced response. Without applying the moments to the beam, these evanescent waves do not vanish. Evidently, the forces can still be tuned to achieve a better approximation of a traveling wave at the center of the beam [9,10]. Nevertheless, the evanescent part, close to the edge, cannot be dealt without using the optimal excitation that includes moments.

4.2 Creating Waves in a Membrane. A membrane can be considered as a two-dimensional string and therefore, evanescent waves do not appear in this structure. A thin rectangular membrane with dimensions $L_1 \times L_2$ and density per unit thickness ρ is stretched by a uniform tension per unit length T . The equation of motion is described by the two-dimensional wave equation [23]:

$$T \left(\frac{\partial^2 u}{\partial x^2} + \frac{\partial^2 u}{\partial y^2} \right) - \rho \frac{\partial^2 u}{\partial t^2} = f(x, y, t) \quad (62)$$

The membrane is modeled by an FE model having mass and stiffness matrices \mathbf{M}, \mathbf{K} , respectively [22]. The external forces \mathbf{F} are applied to the nodes, and q_n is the deflection of the n th node located at (x_n, y_n) . A two-dimensional pure traveling wave in the membrane has the form,

$$u_{tw}(x, y, t) = C_0 e^{-i(\kappa_x x + \kappa_y y)} e^{i\omega t} \quad (63)$$

Rather than a single wavenumber, the wave is described here by a wave vector, $\boldsymbol{\kappa}$ as follows:

$$\boldsymbol{\kappa} = \begin{bmatrix} \kappa_x \\ \kappa_y \end{bmatrix} \quad (64)$$

The two-dimensional wave has a wavelength $\lambda = 2\pi / \|\boldsymbol{\kappa}\|$, and it travels in a direction γ , which is determined by the angle (relative to the x -axis):

$$\gamma = \tan^{-1} \left(\frac{\kappa_y}{\kappa_x} \right) \quad (65)$$

4.2.1 Describing Planar Traveling Waves Using the Modes of the Membrane. Membrane and plate modes are usually denoted by two indices indicating the two directions in plane, i.e., ϕ_{mn} [23]. Figure 5 shows the nine initial modes of an example membrane, calculated from its FE model. Choosing a desired traveling wave response (i.e., wavelength and direction of travel in plane), the modal coefficients may be calculated using Eq. (52). The modal coefficients are presented on the (m, n) plane in Fig. 6 for several wavelengths and wave directions. It is possible to see that differ-

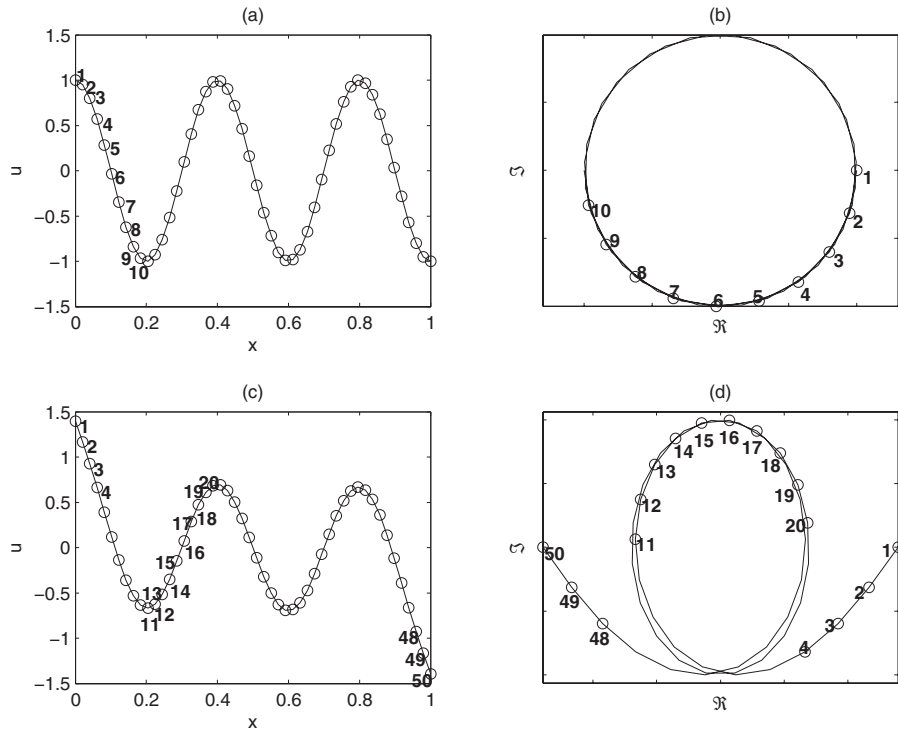


Fig. 4 Beam's spatial response (a) and (c), and complex amplitude (b) and (d). The numbers indicate the measured points and the corresponding locations on the complex amplitude. (a) and (b) The response to the optimal excitation (a pure traveling wave). (c) and (d) The response to the forces only (without moments).

ent modes become significant for different wavelengths. Moreover, a different group of modes can become significant when the direction of the wave's propagation is changed since the effective wavelength of each mode changes with the observation angle in the x - y plane.

4.2.2 Visualizing Planar Vibrations and Waves Using Power-Flow. Inspecting planar vibrations of a two-dimensional structure and being able to quantify how close are the vibrations to a traveling wave is not a straight forward task in this case. One possible way to illustrate traveling waves is to use animation; this is unusable when showing static images. A different way to illus-

trate a propagating phenomenon is to present the power-flow of the vibrations. Waves carry energy in the direction of the propagation [14,24]. The closer the vibrations are to a pure propagating wave, the more power flows with the wave. On the other hand, the mean power-flow per period is zero when the wave is standing. In the general case, power flows in all directions and in different amounts. In this work, the results of the two-dimensional waves are presented by using the mean power-flow per period of the generated structural vibrations.

4.2.3 Solving the FE Model. Setting the desired traveling wave's parameters for Eq. (63) and using the membrane's FE model, the forces needed to be applied to the membrane are cal-

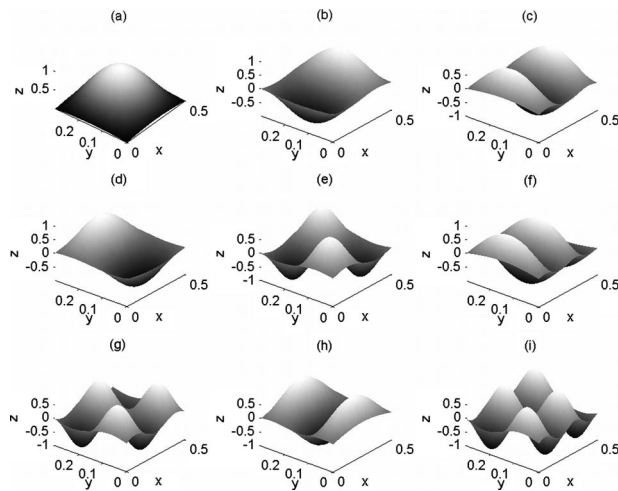


Fig. 5 Nine initial modes of the membrane in the example: (a) ϕ_{11} , (b) ϕ_{21} , (c) ϕ_{31} , (d) ϕ_{12} , (e) ϕ_{22} , (f) ϕ_{14} , (g) ϕ_{32} , (h) ϕ_{13} , and (i) ϕ_{41}

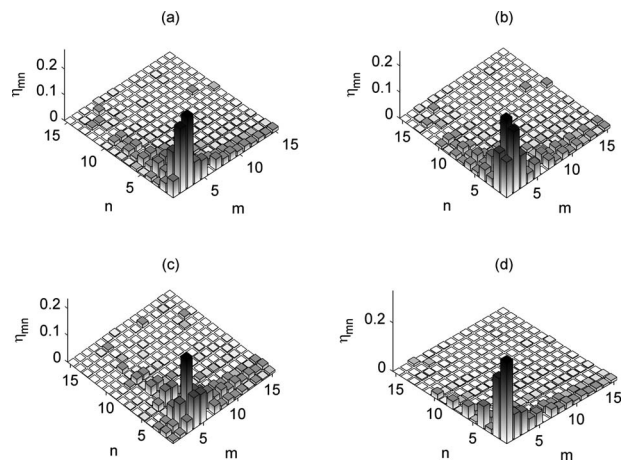


Fig. 6 Modal coefficients for different wavelengths and wave directions: (a) $\lambda=0.4$ $\gamma=25$ deg, (b) $\lambda=0.4$ $\gamma=50$ deg, (c) $\lambda=0.2$ $\gamma=35$ deg, and (d) $\lambda=0.7$ $\gamma=75$ deg

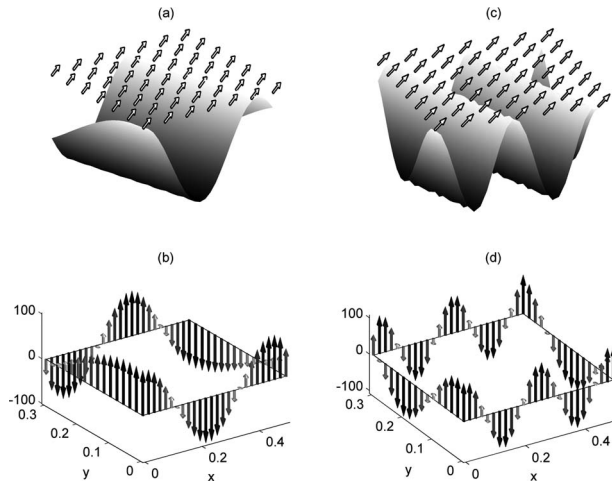


Fig. 7 (Top images) Membrane's vibration and the corresponding mean power-flow (marked by arrows) and the matching force distribution (bottom images). (a) and (b) $\lambda=0.4$ $\gamma=25$ deg, and (c) and (d) $\lambda=0.2$ $\gamma=35$ deg.

culated (using Eq. (57)). The resulting force shape appears to be the extension of the string/beam results. The results show that forces need only to be applied along the edges of the membrane in order to generate a desired traveling wave. Figure 7 shows the resulting force distribution and the membrane's response for two different wavelengths and direction of propagation. The response power-flow has a single direction and uniform intensity, indicating that indeed the generated response is a traveling wave. The forces along the edges follow a pattern of a propagating wave along each edge.

Selecting the ten most significant modes of the membrane from Fig. 6(a), the response and the required forces are calculated. The calculated response and the force distribution are shown in Figs. 8 and 9. Comparing the membrane's response with the response shown in Fig. 7(a), it is possible to see that in a large region on the center of the membrane the response is close to a pure traveling wave (most of the power flows in a single direction), while the edges of the membrane are vibrating in standing wave pattern. Clearly, the truncated model leads to the conclusion that the forces must be applied along the entire structure and not only at the edges of the membrane.

4.2.4 Comparing With a Direct Analytical Solution. Knowing the fact that forces must be applied only along the edges of the membrane, in order to excite a desired traveling wave, the relative time variation in these forces can be computed analytically. The presented method is an extension of the active-sink method [6,9] for two-dimensional structures. Incorporating the forces applied to the membrane at the boundary by imposing suitable boundary

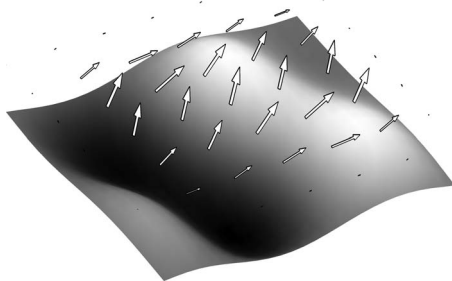


Fig. 8 Membrane response and power-flow obtained by exciting only the ten most significant modes from Fig. 6(a)

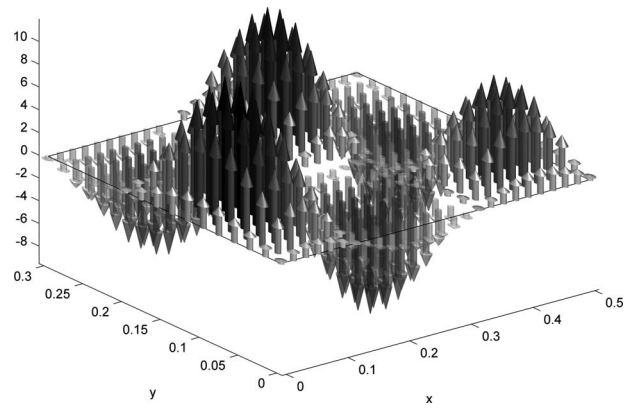


Fig. 9 Force distribution over the membrane calculated to excite the ten most significant modes from Fig. 6(a)

conditions, eliminates the need for right hand terms (forces, e.g., Equation (62)). The boundary conditions for a membrane can be described, in this case, as follows:

$$T \left. \frac{\partial u}{\partial x} \right|_{x=0} = -f_1(y)e^{i\omega t}, \quad T \left. \frac{\partial u}{\partial x} \right|_{x=L_1} = f_2(y)e^{i\omega t}$$

$$T \left. \frac{\partial u}{\partial y} \right|_{y=0} = -f_3(x)e^{i\omega t}, \quad T \left. \frac{\partial u}{\partial y} \right|_{y=L_2} = f_4(x)e^{i\omega t}$$
(66)

Substituting the desired traveling wave in Eq. (63) into Eq. (66) and comparing the coefficients, the forces along the edges are obtained as follows:

$$f_1(y) = iu_0 T \kappa_x e^{-i\kappa_y y}$$

$$f_2(y) = -iu_0 T \kappa_x e^{-i\kappa_x L_1} e^{-i\kappa_y y}$$

$$f_3(x) = iu_0 T \kappa_y e^{-i\kappa_x x}$$

$$f_4(x) = -iu_0 T \kappa_y e^{-i\kappa_y L_2} e^{-i\kappa_x x}$$
(67)

The solution given in Eq. (67) shows that the forces along the edges have a pattern of traveling waves where the effective wavelength along each edge is a projection of the propagating wave. Clearly, this is identical to the solution obtained by the modal summation.

4.3 Nonuniform Structures. The modal approach to excite traveling waves can be applied to complex models of structures where analytical solutions are much harder to obtain. Two examples, of one and two-dimensional structures are shown here to illustrate that even in these cases the proposed method can produce the required force distribution that gives rise to a specified response.

4.3.1 A Discontinuous Beam Example. As a one-dimensional example, a beam having a nonuniform thickness is shown. The beam has thickness h_1 along section of length L_1 and then the thickness changes to h_2 for the rest of the beam's length. Since the excitation frequency is identical for both beam's sections, two different wavenumbers (wavelengths) are expected. One for each section of the beam— κ_1, λ_1 and κ_2, λ_2 , respectively. The ratio between the wavelengths is:

$$\frac{\lambda_2}{\lambda_1} = \frac{\kappa_1}{\kappa_2} = \left(\frac{h_1}{h_2} \right)^2$$
(68)

Building an FE model of a beam, having two sections with two different thicknesses, the forces needed to generate a desired traveling wave response can be calculated using Eq. (57). Figure 10 shows the results of such a calculation and Fig. 11 shows the

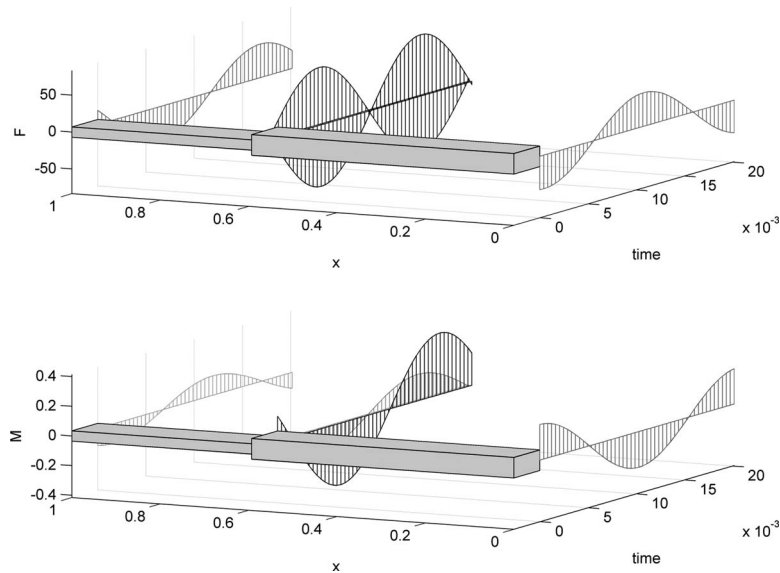


Fig. 10 Force and moment distribution along a beam with an abrupt change in cross section. (Top) force distribution and (bottom) moment distribution.

obtained response. It is shown that along each section of the beam the traveling wave has a different wavelength. It turns out that harmonic forces and moments should be applied only to the beam edges and on the point of discontinuity.

4.3.2 Membrane With a Localized Mass. As an example for a nonuniform two-dimensional structure, a membrane with a localized mass at its center is considered. Once again using a FE model, and applying Eq. (57) to calculate the forces for the desired traveling wave response. Figure 12 shows the resulting forces. It can be seen that similarly to the simple membrane that was shown before, forces along the edges of the membrane should be applied. In addition, a point force is applied at the same location of the added point mass.

5 Conclusion

This work uses a linear combination of the natural normal modes to express the excitation that generates a specified traveling wave. It is shown that the modal approach, although its elements are standing waves, can represent traveling waves and thus it is effective in the process of finding the required force distribution. The presented method can handle complex structures and numerical models to calculate the desired excitation that forms pure traveling waves in any direction in space. The results show that the required excitation is concentrated along the structure's boundaries and at points of discontinuity. When only a few structural modes are considered, an approximate, nonpure traveling wave can still be obtained. The results may have a wider scope than for

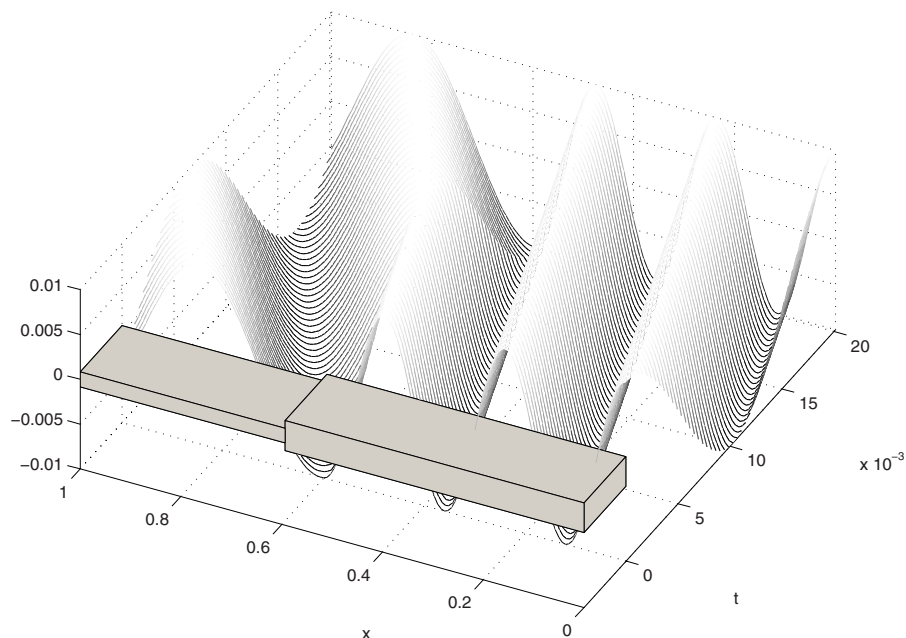


Fig. 11 Traveling wave response of a beam with an abrupt change in cross section

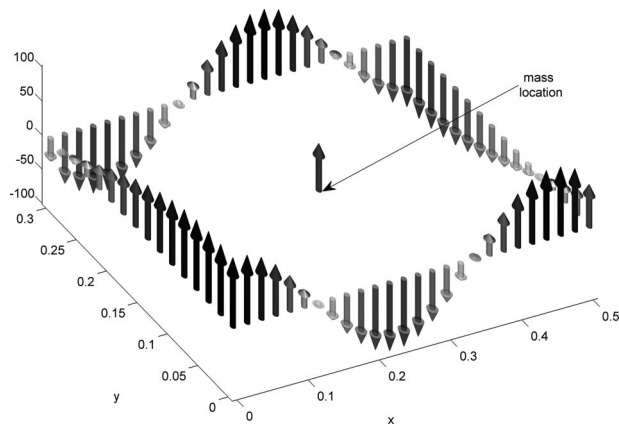


Fig. 12 Distribution of forces generating a pure traveling wave on a membrane with a localized mass

the problem of generating traveling wave and may be related to other problems such as control and cancelation of vibrations. In this respect, the theoretical results that were obtained here clearly help in designing the preferred positions of actuators in several vibration control applications.

Acknowledgment

This research was supported by the Israel Science Foundation under Grant No. 579/04.

References

[1] Mead, D. J., 1996, "Wave Propagation in Continuous Periodic Structures: Research Contribution From Southampton, 1964–1995," *J. Sound Vib.*, **190**, pp. 495–524.

[2] Kuribayashi, M., Ueha, S., and Mori, E., 1985, "Excitation Conditions of Flexural Traveling Waves for a Reversible Ultrasonic Linear Motor," *J. Acoust. Soc. Am.*, **77**, pp. 1431–1435.

[3] Minikes, A., and Bucher, I., 2003, "Non-Contacting Lateral Transportation Using Gas Squeeze Film Generated by Flexural Traveling Waves—Numerical Analysis," *J. Acoust. Soc. Am.*, **113**, pp. 2464–2473.

[4] Chen, L., Wang, Y., Ma, S., and Li, B., 2003, "Analysis of Traveling Wave Locomotion of Snake Robot," Proceedings of the 2003 IEEE, International

Conference on Robotics, Intelligent Systems, and Signal Processing, Changsha, China.

[5] O'Connor, W. J., and Lang, D., 1998, "Position Control of Flexible Robot Arms Using Mechanical Waves," *ASME J. Dyn. Syst., Meas., Control*, **120**, pp. 334–339.

[6] Tanaka, N., and Kikushima, Y., 1991, "Active Wave Control of a Flexible Beam (Proposition of the Active Sink Method)," *JSME Int. J., Ser. III*, **34**, pp. 159–167.

[7] Mace, B. R., 1984, "Wave Reflection and Transmission in Beams," *J. Sound Vib.*, **97**(2), pp. 237–246.

[8] O'Connor, W. J., 2008, "Wave-Based Control of Flexible Mechanical Systems," International Conference on Noise and Vibration Engineering (ISMA2008), Leuven, Belgium.

[9] Gabai, R., and Bucher, I., 2009, "Excitation and Sensing of Multiple Vibrating Traveling Waves in One-Dimensional Structures," *J. Sound Vib.*, **319**, pp. 406–425.

[10] Minikes, A., Gabay, R., Bucher, I., and Feldman, M., 2005, "On the Sensing and Tuning of Progressive Structural Vibration Waves," *IEEE Trans. Ultrason. Ferroelectr. Freq. Control*, **52**, pp. 1565–1576.

[11] Manceau, J. F., and Bastien, F., 1995, "Production of a Quasi-Traveling Wave in a Silicon Rectangular Plate Using Single Phase Driver," *IEEE Trans. Ultrason. Ferroelectr. Freq. Control*, **42**, pp. 59–65.

[12] Bucher, I., 2004, "Estimating the Ratio Between Traveling and Standing Vibration Waves Under Non-Stationary Conditions," *J. Sound Vib.*, **270**, pp. 341–359.

[13] Feeny, B. F., 2006, "A Method of Decomposing Wave Motions," Proceedings of the ASME IMECE'06, Chicago, Nov. 5–10.

[14] Achenbach, J. D., 1973, *Wave Propagation in Elastic Solids*, North-Holland, Amsterdam.

[15] Norton, M. P., 1989, *Fundamentals of Noise and Vibration Analysis for Engineers*, Cambridge University Press, Cambridge, UK.

[16] Levitan, B. M., 1987, *Inverse Sturm-Liouville Problems*, VNU Science, Utrecht, The Netherlands.

[17] Bishop, R. E. D., Gladwell, G. M. L., and Michaelson, S., 1965, *The Matrix Analysis of Vibration*, Cambridge University Press, Cambridge, UK.

[18] Spiegel, M. R., 1952, "The Dirac Delta-Function and the Summation of Fourier Series," *J. Appl. Phys.*, **23**, pp. 906–909.

[19] Noble, B., and Daniel, J. W., 1988, *Applied Linear Algebra*, 3rd ed., Prentice-Hall International, Englewood Cliffs, NJ.

[20] Bucher, I., and Braun, S. G., 1997, "Left-Eigenvectors: Extraction From Measurements and Physical Interpretation," *Trans. ASME, J. Appl. Mech.*, **64**(1), pp. 97–105.

[21] Geradin, M., and Rixen, D., 1997, *Mechanical Vibrations: Theory and Application to Structural Dynamics*, Wiley, Chichester.

[22] Cook, R., Malkus, D. S., Plesha, M. E., and Witt, R. J., 2002, *Concepts and Applications of Finite Elements Analysis*, Wiley, New York.

[23] Morse, P. M., 1986, *Vibration and Sound*, McGraw-Hill, New York.

[24] Cremer, L., Heckl, M., and Ungar, E. E., 1973, *Structure-Borne Sound: Structural Vibrations and Sound Radiation at Audio Frequencies*, Springer-Verlag, Berlin.